IOP Conf. Series: Journal of Physics: Conf. Series **1272** (2019) 012017 doi:10.1088/1742-6596/1272/1/012017

# PCB-3D-Printed, Reliable and Reusable Wells for Impedance Spectroscopy of Aqueous Solutions

**J J Cabrera-López[1, 2], M F García-Arrunátegui[1], P Neuta-Arciniegas[1], O Campo[1] and J Velasco-Medina[2]**

[1] Research Group on Biomedical Engineering. Universidad Autónoma de Occidente (Valle) Colombia
[2] Research Group on Bionanoelectronics. Universidad del Valle (Valle) Colombia

E-mail: jjcabrera@uao.edu.co

**Abstract**. Impedance Spectroscopy (IS) has been shown to be a non-invasive and reliable technique for the electrical characterization of biological materials. This paper presents the design and implementation of reliable, reusable wells that are used to perform IS measurements of aqueous solutions. These reusable wells are detachable, easy to clean and low-cost and they are made up of a platen on a Printed Circuit Board (PCB) and the chambers are manufactured using 3D-printing technology. In this case, in order to verify its functionality, IS measurements of electrolytic and non-electrolytic aqueous solutions were carried out. Initially, as a reference, the impedance spectrum of a Hanks' solution was obtained following a proposed measurement protocol. Then, we analyse this spectrum and we propose an Equivalent Electrical Model (EEM) for validating the reusable wells. Finally, IS measurements are carried out on aqueous solutions of molecular D-glucose and sodium chloride prepared in Hanks' solution and deionized water, by considering physiological concentrations. The parameter values of the EEMs of each solution tested were obtained using genetic algorithms and Matlab and, from these values, it is possible to conclude that the measurements performed are unable to differentiate the physiological concentration of glucose in the aqueous solution used. Also, from these results, it can be concluded that the designed wells are suitable for IS measurements of aqueous solutions and that they can be used in Electrical Cell Impedance Sensing (ECIS) or applications that require electrical characterization of solutions.

## 1. Introduction

Impedance is the characteristic of materials to avoid the pass of the electric current flow through them [1]. All materials drain and store energy, so impedance is defined regarding resistance and reactance, where the former represents the property of the material to dissipate energy and the latter to store it [2].

The Impedance Spectroscopy (IS) technique consists of injecting an Alternating Current (AC) signal into a Material Under Test (MUT) using a pair of electrodes. Then it is possible to measure a voltage differential signal in the MUT which enables its impedance to be calculated using Ohm's law [1]. Commonly, the AC injected signal is monotonic and a frequency sweep is performed to find the electrical response of the MUT as a function of the frequency. When the MUT is a biological material, the IS technique is known as the bioimpedance technique. Bioimpedance has been widely used to measure body composition[2], estimate the electrical behaviour of extracellular and intracellular

fluids[3] and changes in the volume of tissues [4], as well as for the electrical characterization of tissues[5]. Despite the simplicity of the bioimpedance set up, the measurements may be affected by the temperature of the MUT[6], its thermodynamic equilibrium and electrode/electrolyte interface balance [7], [8] as well as the stabilization time of the sample[9]. Therefore, if a measurement protocol is not carefully designed and scheduled, the measurement results can be misinterpreted and lead to faulty conclusions.

On the other hand, 3D printing is defined as a manufacturing process by addition of material. In this process, objects are created by adding material layer by layer from a digital model. One of the best known 3D printing techniques is the Fused Deposition Modelling (FDM). In this process, a filament of polymeric material is introduced into the pre-heated nozzle of a 3D printer and the melted material is extruded over a scaffold. The extruded material solidifies after a few seconds and the track filled by this material builds a layer of the object. Then, the next layer is extruded and the process continues until the whole object is printed. 3D printing processes have been used in industrial [10] and biomedical applications [11] and automotive manufacturing [12]. For example, in [13], the authors use FDM to build test phantoms of a tank and skull for electrical impedance tomography.

In this paper, we present the design and implementation of detachable, easy to clean, low-cost and reusable wells that can be used to perform IS measurements of aqueous solutions. In this case, the reusable wells were manufactured using 3D-printing technology and a Printed Circuit Board (PCB), and its functionality was validated using the proposed Equivalent Electrical Model and IS measurements of electrolytic and non-electrolytic solutions.

The remainder of the paper is organized as follows: Section 2 describes the design of the reusable wells, the measurement protocol and the proposed EEM. Section 3 presents the experimental results of the IS measurements. Section 4 discusses these results and, finally, the conclusions are presented in Section 5.

## 2. Design and validation of the experimental set-up

The design of the reusable wells and the proposed IS measurement protocol are presented in this section. Also, we explain the experimental results of IS measurements obtained from the standard Hanks' solution and the EEM proposed for the designed reusable wells.

### *2.1. 3D-printed reusable wells*

Here, we present the design and implementation of a device with four reusable wells suitable for IS measurements of aqueous solutions. The framework of this device is composed of three detachable pieces as shown in Figure 1(a). The support piece, or platen of the wells, is made on a PCB, in whose top layer have been a printed tetrapolar array of gold-coated electrodes as shown in Figure 1(b). The middle piece of the framework is composed of four type O-Rings ¾ inch seals that guarantee the hermetic sealing of each well. The upper piece of the device corresponds to the walls of the wells or the chamber that was manufactured using a 3D-printer. In this case, the GigaBox 360, an FDM 3D-printer and the Acrylonitrile Butadiene Styrene (ABS) material were used to create this chamber. Although Polylactic Acid (PLA) is one of the most commonly used materials in these manufacturing techniques, we selected ABS because it is not biodegradable compared with PLA and it has a useful property to mitigate its degradation when it is in contact with the aqueous solutions. The setup parameters for 3D printing of the chamber were 20% infill and walls of 0.8 mm thin. The Z layer height was set to 0.1 mm and the geometry of the wells was designed for no supports in the printing process. In this way, the printed chamber is a quadrilateral of 80 by 80 mm and 10 mm depth and the wells are 16 mm in diameter and the printing process time was 2.5 hours. Also, this printing chamber has two snap-on brackets which were designed to clamp the PCB, the O-Rings and chamber, achieving a watertight unit. The snap-on brackets allow easy disassembly of the chamber for cleaning purposes using ultrasonic washing.

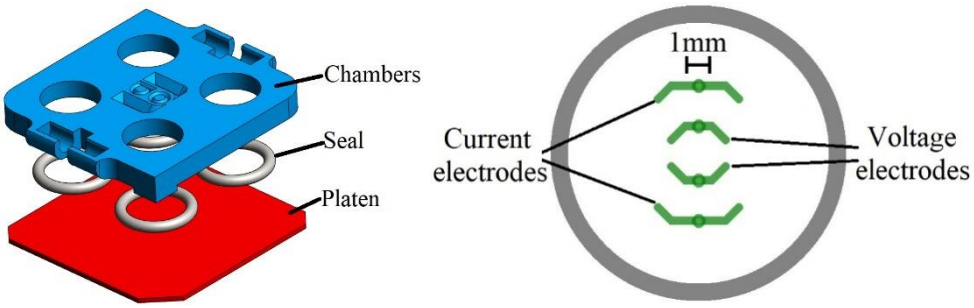


**Figure 1.** Reusable 3D-Printed wells. (a) Exploded view of the device with four wells for IS measurements of aqueous solutions and (b) top view of the electrode array of one well.

### *2.2. Aqueous Solutions and IS Measurement Protocol*

In order to perform the IS measurements and the functional validation of the designed device, as a buffer medium and reference solution, we use the Hanks' balanced salt solution without phenol red (by LONZA), and three different groups of aqueous solutions. The first one consists of eight solutions with different physiological concentrations between 4.0 and 6.0 mmol/L of molecular D-glucose (MERCK KGaA) which was dissolved in Hanks' solution; the second one consists of three solutions of Hanks' with growing concentrations of sodium chloride of between 0.1 M and 0.15M (including Hanks´ standard concentration of 0.13M); and the third one consists of three solutions of sodium chloride diluted in deionized water using the same concentrations as in group 2. In order to ensure that the thermodynamic equilibrium between the wells and the sample is reached quickly at the time of the IS measurements, these three groups of aqueous solutions were kept at room temperature in dark amber glass bottles.

We empirically adjust a protocol for IS measurements, using [1] and [2] as references. This proposed protocol consists of four steps: The first one performs the washing, cleaning and drying of the reusable wells using deionized water and absorbent paper towels; the second performs the addition of 1 ml of the aqueous solution into each well, as shown in Figure 2; The third is to keep the device of the reusable wells with the aqueous solutions in each well in a controlled environment (25 °C and 60% RH), to achieve the thermodynamic equilibrium and stabilization of the electrode-solution interface; and the fourth step carries out the IS measurements. Then, we record ten spectra of each aqueous solution under test, to validate the repeatability of the measurements.

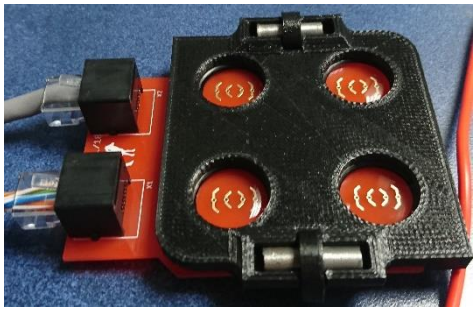

**Figure 2.** Four 3D-printed reusable wells, each one with 1 ml of an aqueous solution.

Finally, we perform IS measurements of the Hanks' solution using an enhanced version of the CoreBioZ system [1] and the reusable wells. This enhanced system works in the bandwidth between 100 Hz and 100 KHz using a tetrapolar arrangement of electrodes [14]. Then, using the proposed measurement protocol, the plot of the impedance magnitude shown in Figure 3 was obtained. In this case, very small variations of the order of the units are observed for the impedance magnitude in the

bandwidth of the IS measurements. Therefore, the impedance can be considered constant in the measured spectrum. This result is coherent with expectation because Hanks' is a nonelectrolyte solution; hence its impedance does not depend on the frequency. In this way, the developed, reusable wells can be functionality validated.

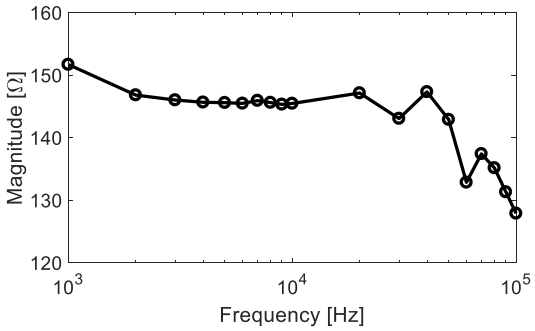


**Figure 3.** Bode plots for Hanks' solution (buffer solution).

However, to describe the slope at the high-frequency of the IS measurements for the Hanks' solution (Figure 3), we propose an EEM like the one shown in Figure 4. In this case, a resistor $R_s$ and parallel $RC$ circuits model the aqueous solution and the interfaces, respectively. These interfaces are created in the transition zone between a metal (electrode) and a polar solution (such as Hanks'), whereby migration and diffusion phenomena during the time of thermodynamic equilibrium create the effects of a double layer, which have been represented by resistors $R_{dl}$ and capacitors $C_{dl}$ [14].The validation of the EEM proposed is presented in the next section using additional experimental results.

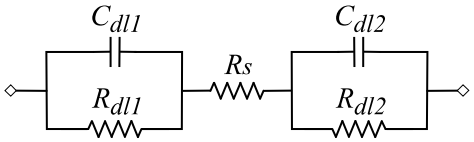


**Figure 4.** The proposed EEM for polar solution IS measurements using the reusable wells.

## 3. Experimental Results

In this section, we present the experimental results obtained from the IS measurements using the three aqueous solutions mentioned above. In order to obtain the experimental results and to validate their repeatability, ten impedance spectra of each test solution were recorded using the enhanced CoreBioZ.

Initially, we analyze the experimental results obtained from the Hanks' solutions and deionized water, with diluted concentrations (0.1, 0.13 and 0.15 M) of sodium chloride; that is, the solutions of groups 2 and 3.For the concentration of 0.13 M of the solutions of these two groups, Figure 5 shows the average of the spectra obtained and, from these spectra, we found that the maximum standard deviation is less than 5 **Ω**, and the high repetitiveness of the experimental set-up can be ensured. Also, from these spectra, we found a similar waveform as the Hanks' solution spectrum showed in Figure 3, achieving small variations in the impedance magnitude. Then, we can use the proposed EEM to describe the electrical behavior of the aqueous solution in the reusable wells. Table 1 presents the parameter values of the EEM obtained using a genetic optimization algorithm[15] and the spectra of Figure 5.From this table, it is possible to mention that the capacitances($C_{dl}$) and resistances($R_{dl}$) that model the double layer effects of the electrode/solution interface have close values between them and keep the order of magnitude. Also, the impedance value of the aqueous solution under test, modeled by $R_s$, decreases when the concentration of sodium chloride rises, because the solution becomes more conductive. The

simulation results using the parameter values are presented in Figure 5 as a dashed line. According to the NRMSE estimator index, the goodness of fit between these simulations and experimental results are above 0.92 and, thus, we can accept the parameter values obtained and validate the proposed EEM.

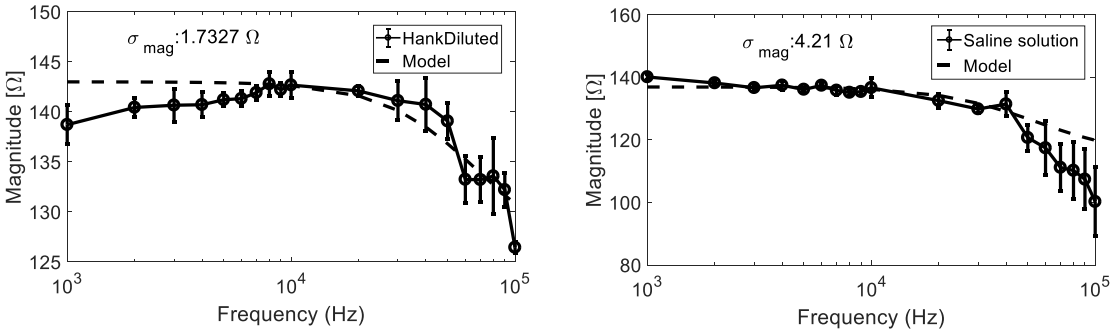


**Figure 5.** Spectra of the magnitude of the impedance for Hanks' and deionized water solutions with dilute sodium chloride.

Then, we analyze the experimental results obtained from solutions prepared with Hanks' buffer and dissolved D-Glucose. In this case, we considered the eight physiological concentrations of D-Glucose used in [16], and we found that the impedance magnitude spectra do not show significant variations that allow differentiating between the D-Glucose concentrations analyzed. In Figure 6, the average spectrum of the eight glucose concentrations that were analyzed are presented in a solid line, on which the error bars show the low variability obtained from these eight spectra. Also, from this Figure, we observe that the obtained spectrum preserve the waveform as the above-presented spectra and, therefore, we can consider the EEM proposed, finding that the parameter values calculated for this model are very close to those obtained for Hank's buffer with 0.13 M of sodium chloride. The simulation result using the parameter values is plotted as a dashed line in Figure 6, and the calculated value of 0.94 for the NRMSE estimator indicates a high correlation between this result and the average spectrum (solid line).

**Table 1.** Parameter values of the EEM.

| Sodium chloride dissolved in | Concentration $[M]$ | $R_{dli}[\Omega]$ | $C_{dli}[\mathrm{F}]$ | $R_s[\Omega]$ |
|---|---|---|---|---|
| Hanks' buffer | 0.1 | 12 | 1.72E-7 | 132 |
| | 0.13 | 9 | 2.72E-7 | 125 |
| | 0.15 | 10 | 1.88E-7 | 120 |
| Deionized water | 0.1 | 10 | 2.81E-7 | 120 |
| | 0.13 | 11 | 2.80E-7 | 114 |
| | 0.15 | 11 | 1.65E-7 | 110 |

$i = \{1,2\}$

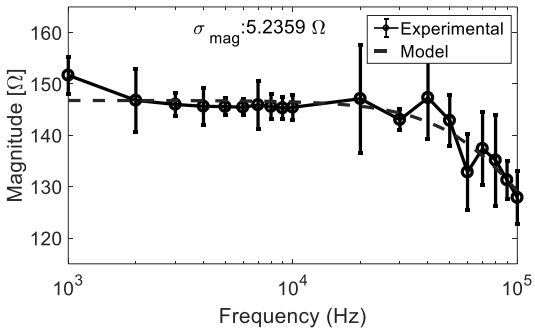


**Figure 6.** Bode plots for all concentrations.

## 4. Discussion

From the experimental results obtained using IS measurements, we can conclude that the aqueous solutions studied show resistive behavior, as expected, and that the measurement set-up can be emulated using the proposed EEM. The calculated parameter values for this model, in each case studied, are consistent, especially if we observe that $R_s$ decreases when the conductivity increases due to the rise in the concentration of the electrolyte (sodium chloride). Also, we found that, following the IS measurement protocol proposed, it is not possible to differentiate between the physiological concentrations of glucose when it is dissolved in Hanks' buffer; contrary to the results presented in [16] where the authors claim that the impedance of the solution decreases when the glucose concentration increases. We consider that our results are valid because glucose is a nonelectrolyte solute. This means that glucose is a soluble substance which can be dissolved in Hanks' buffer and it doesn't modify the solution impedance because it doesn't generate ions. Instead of this, covalent bonds are created in the solution, which are characterized as not being conductors of electricity.

In contrast, sodium chloride is an electrolytic substance which can be dissolved in water forming sodium and chloride ions with positive and negative charges, respectively. Therefore, the electrical characteristics of the formed solution allow the conduction of the current to a greater or lesser degree, depending on the concentration of this solute; as was observed in the results presented when this solute is dissolved in deionized water or Hanks' buffer.

Finally, the results confirm that the measurement set-up is reliable and highly repeatable and the reusable wells do not react with the aqueous solutions nor do they change their electrical characteristics, even if the concentrations of solutes are modified.

## 5. Conclusions

In this work, we developed PCB-3D-printed, reusable wells for impedance spectroscopy of aqueous solutions. The wells were especially fabricated with non-biodegradable materials, suitable for aqueous solutions. The fabrication method proposed in this paper may be adapted to other conditions for manufacturing wells for research on impedance spectroscopy.

This work concluded that glucose determination in terms of impedance using Hanks' solution was not reliable for a physiological range. That is, it is not possible to measure glucose directly by bioimpedance because it doesn't allow current flow, though not being an electrolytic solute.

The designed wells are suitable for IS measurements of aqueous solutions and they can be used in applications that require electrical characterization and ECIS, as can be concluded from the measurements taken.

It is important to take into account factors that affect the measurements in order to control these for example, temperature as if this decreases, ions lose mobility and increase conductivity. Also, to obtain repeatability and reliable results it is important to design a specific experimental protocol, to standardize the time of the solution in the wells and that in this way the thermodynamic equilibrium in the electrolyte-electrode is guaranteed.

**References**

[1] Cabrera J J, Velasco J, Denis E, Calderon J F B and Guevara O J G 2016 Bioimpedance measurement using mixed-signal embedded system *IEEE 7th Latin American Symposium on Circuits & Systems (LASCAS)* 335-8
[2] Gonzalez C 2018 Body composition by bioelectrical impedance analysis *Bioimpedance in Biomedical Applications and Research* 219-41
[3] Freeborn T J, Maundy B and Elwakil A S 2014 Extracting the parameters of the double-dispersion cole bioimpedance model from magnitude response measurements *Med. Biol. Eng. Comput.* **52** 749-58
[4] Dai T and Adler A 2009 In vivo blood characterization from bioimpedance spectroscopy of blood pooling *IEEE Trans. Instrum. Meas.* **58** 3831-8
[5] Qiao G, Wang W, Duan W, Zheng F, Sinclair J and Chatwin C R 2012 Bioimpedance analysis for the characterization of breast cancer cells in suspension *IEEE Trans. Biomed. Eng.* **59** 2321-9
[6] Olmo A, Buzón B, Yúfera A and Risco R 2010 Bioimpedance monitoring for cryopreservation process control *2010 Annu. Int. Conf. IEEE Eng. Med. Biol. Soc. EMBC'10* 6555-8
[7] Lima L F, Vieira A L, Mukai H, Andrade C M G and Fernandes P R G 2017 Electric impedance of aqueous KCl solutions: salt concentration dependence on component of the equivalent electric circuit *J. Mol. Liq.* **1** 1-29
[8] Mirtaheri P, Grimnes S and Martinsen O G 2005 Electrode polarization impedance in weak NaCl aqueous solutions *IEEE Trans. Biomed. Eng.* **52** 2093-9
[9] McAdams E 2014 Bio-impedance spectroscopy problems to avoid *Int. Conf. Des. Technol. Integr. Syst. Nanoscale Era* 1-2
[10] Petrovic V, Haro V, Jordá O, Delgado J, Blasco J R and Portolés L 2011 Additive layered manufacturing: sectors of industrial application shown through case studies *Int. J. Prod. Res.* **49** 1061-79
[11] Yan Q, Dong H, Su J, Han J, Song B, Wei Q and Shi Y 2018 A Review of 3D printing technology for medical applications *Engineering. Elsevier Ltd.* **4** 729-42.
[12] Bogue R 2013 3D printing: the dawn of a new era in manufacturing? *Assem. Autom.* **33** 307-11
[13] Avery J, Aristovich K, Low B and Holder D 2017 Reproducible 3D printed head tanks for electrical impedance tomography with realistic shape and conductivity distribution *Physiol. Meas.* **38** 1116-31
[14] Hegarty M, Grant E and Reid L 2015 A wearable bioimpedance spectroscopy system for characterizing fluid distribution in the lower limbs *IEEE Int. Conf. Multisens. Fusion Integr. Intell. Syst.* 328-33
[15] Kazilas M, Skordos A and Partridge I K 2005 Parameter estimation in equivalent circuit analysis of dielectric cure monitoring signals using genetic algorithms *Inverse Problems in Science and Engineering* 157-76
[16] Kamat D K, Bagul D, and Patil P M 2014 Blood glucose measurement using bioimpedance technique *Adv. Electron.* 4-9